Design and pre-evaluation of a backward facing step experiment with liquid metal coolant

W. Jaeger[1], T. Schaub Hahn[1], W. Hering[1], I. Otic[1], A. Shams[2], J. Oder[3], I. Tiselj[3]

[1]Karlsruhe Institute of Technology, Germany

wadim.jaeger@kit.edu, thomas.schaub@kit.edu, wolfgang.hering@kit.edu, ivan.otic@kit.edu

[2]Nuclear Research and Consultancy Group (NRG), The Netherlands

shams@nrg.eu

[3]Jozef Stefan Institute, Slovenia

jure.oder@ijs.si, iztok.tiselj@ijs.si

ABSTRACT

This paper summarizes the efforts in designing and pre-evaluating a vertical backward facing step (BFS) experiment, with liquid sodium flow. Conducting such study is important, since sudden geometrical variations, e.g., in a flow channel, impacts the thermal-hydraulic behavior. Geometrical variations occur many times in manifolds, heat exchangers or fuel bundles. Hence, it is reasonable to investigate their influence on the flow. Up to now, the information related to backward facing steps with liquid metal coolant is sparse. The majority of investigations related to backward facing steps have been performed with fluids like air or water. Due to the fundamental differences between fluids with a Prandtl number around unity, like water and air, and fluids with a very small Prandtl number, like sodium, a one-to-one transfer of knowledge from one fluid group to another is impossible. In addition, experimental and numerical studies related to liquid metal thermal hydraulics are focusing on homogenous geometries like pipes, ducts or rod bundles, not considering the influence of geometrical variations along the flow channel. In the frame of the EU Horizon 2020 project SESAME, an extensive effort has been put forward to study the vertical BFS case. The main idea is to generate a reference database in order to validate and improve the pragmatic turbulence modelling approaches for such flow configurations. Therefore, an experimental study is foreseen to be performed with liquid sodium. In addition, a complimentary DNS of a similar geometry configuration will be performed. In the context of this study, a combined effort of the experiments, DNS, LES and RANS modelers will be put forward in order to design a vertical BFS with liquid sodium. Different aspects of the BFS design are studied to make a suitable and well-defined reference database. To name a few, the influence of the corner design of the rectangular ducts is studied. Furthermore, the estimation of the entrance length and the recirculation zone is part of this investigation, which will be valuable in placing the measurement devices at the right positions.

1.   Introduction

The use of benchmark cases for CFD code validation is one of the main reasons why computational simulations of physical phenomena have continuously improved and gained credibility along the years [1]. One of the benchmark test cases for CFD code validation is the backward facing step. The backward facing step is a typical geometrical variation along a flow channel, which can be encountered in the inlet and outlet region of heat exchangers, manifolds, fuel assemblies, etc. Hence, it is interesting to study the influence of the buoyancy in the case where the reattachment zone of the backward facing step is heated. Due to the very particular thermal-hydraulic properties of liquid metals (Pr << 1), this buoyancy effect is of interest, because liquid metals are intended to be used as working fluids for the heat transfer in different power plants (concentrated solar power, fusion and fission nuclear power plants).

In the framework of the SESAME project (thermal hydraulics Simulations and Experiments for the Safety Assessment of MEtal cooled reactors) an extensive effort has been put forward to generate a comprehensive reference database in order to validate available RANS CFD models under buoyant conditions [2]. The work presented in this article is one such example. However, it is worth reminding that in Europe, consensus was achieved that further development of models should be limited [3]. Hence, the main focus should be on the further validation and, if required, the calibration of the available turbulence heat flux models for natural, mixed and forced convection regimes. In this regard, the following promising models have been identified for further validation [4]: AHFM-NRG [5]; Local turbulent Prandtl number modelling and the Turbulence Model for Buoyant Flows (TMBF) [6]. A number of well renowned institutes and companies are involved in this validation procedure (ASCOMP, KIT, NRG, SCK·CEN, VKI). In addition, different CFD will be used, which will provide a road map into the understanding of these aforementioned models.

In this context, the backward facing step experiment is being planned and designed at the INR (KIT). It will be performed in the KASOLA facility [7] in order to provide experimental data for CFD code validation to the scientific community. The current design of the BFS is depicted in Figure 1. KASOLA experiment will be performed with forced sodium flow at low Reynolds numbers with heaters positioned at various segments of the BFS section. The effects of buoyancy are expected to have a strong impact on the flow and heat transfer.

The intention of this paper and the intention of the SESAME project can be condensed to the following process: Application of isothermal RANS CFD for the design of the backward facing step ➔ Construction and operation of the backward facing step ➔ Provision of experimental data to validate and improve RANS CFD under buoyant condition ➔ Comparison of experimental data, RANS CFD results, LES results and direct numerical simulations to each other.
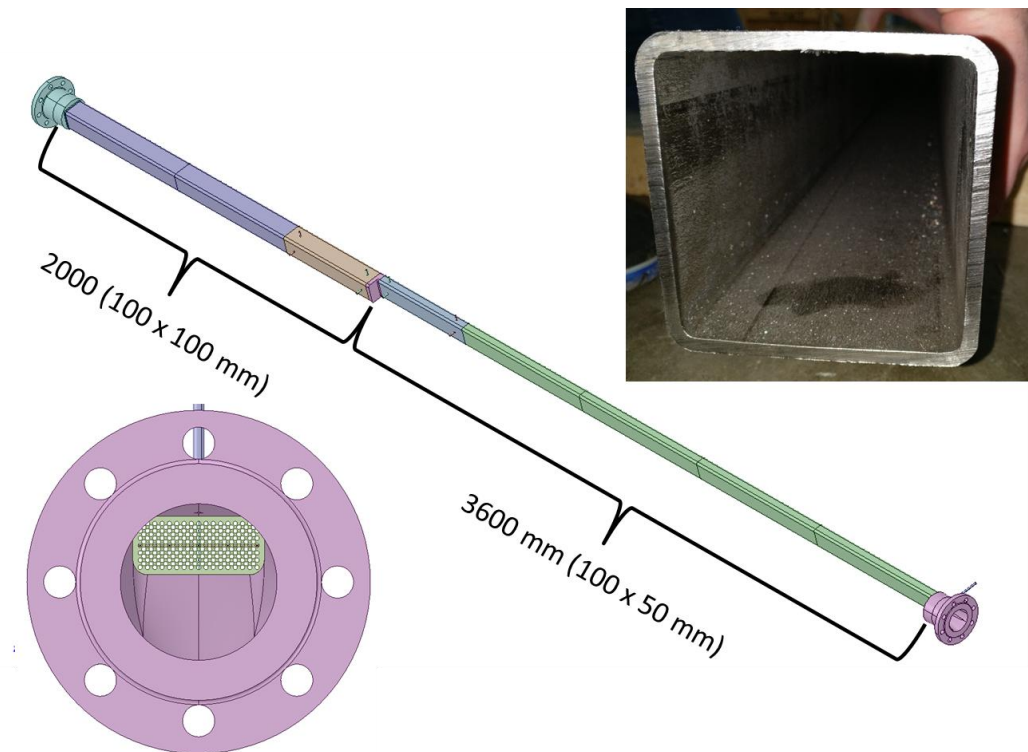
Figure 1 Design of the BFS: Lower left - Transition from circular to rectangular channel with hole plate; Center - BFS test section with dimensions; Top right - Quadratic section of the BFS with rounded corner

2.   The backward facing step design approach

In order to guarantee uniform flow characteristics at the backward facing step and to isolate the backward facing step from any upstream experimental components as far as possible, a flow conditioning section has been incorporated into the KASOLA facility before the backward facing step. A preliminary CFD study of the entrance region becomes very helpful when pretending to optimize and assess different flow conditioning setups and their technical and economic impact in the research project. Considering, that due to spatial reasons the length of the flow conditioning section cannot be modified, special attention has to be put into flow conditioning hardware (grids, screens, honeycombs, hole plates etc.). This, considering that the position of the MHD pump is just before the developing section (distorted velocity layer profiles) and that a round-to-square cross-section adapter is installed, which also acts as a nozzle, since the round piping cross-section is larger than the rectangular duct´s cross section. A detailed introduction into the topic of flow conditioning can be found in Loehrke and Nagib [8], Laws and Livesey [9] and Roach [10].

The manufacturing of a 3600 mm long, perfectly straight, rectangular cross section of 100 x 50 mm with a wall thickness of 5 mm with sharp 90° corners can be very challenging, time and money consuming. The alternative of using commercial rectangular and square ducts with

rounded corners is attractive. Thereby, the radius of the rounded corners is two times the wall thickness. The differences between sharp edged corners and rounded corners with respect to secondary motions must be evaluated. Considering the present status in the development of the KASOLA facility, the best and simplest choice for flow conditioning hardware are hole plates.

Measurements are planned for at least three temperatures (150°C, 200°C and 250°C). Due to the change of thermo-physical properties between 150 and 250°C the Reynolds number increases by 35%, just by means of the varying kinematic viscosity for the given temperature range. This effect must be considered when evaluating the entrance length.

No quantitative conclusions may be taken from these simulations, because this is a preliminary and a qualitative study. The aim is to study behavioural differences when taking different parameters into account, not to make definite quantitative conclusions. Nevertheless, in order to at least roughly validate the CFD simulation, empirical correlations for the pressure drop along the duct are taken from Kakac et al. [11]. White [12] presents an approximate method for calculating the maximum velocity in a turbulent boundary layer from the friction factor. The CFD results are also compared to these calculated velocities. It has to be said that this method is derived with help of the law of the wall and considering an integration process for a circular pipe, which is a very rough approximation for this case (rectangular duct with rounded corners with the presence of secondary motions). But for basic engineering purposes, it may be used as an order of magnitude approximation.

The transfer of correlations and equations of circular pipes for rectangular ducts is made by the use of the hydraulic diameter. The use of a laminar equivalent diameter appears to be a better choice for the hydraulic diameter, especially, when taking empirical correlations derived from experiments with circular pipes as pointed out in [11].

3.   RANS simulation for design optimization

Simulations with the SST (Shear Stress Transport) and the BSLRSM (Baseline Reynolds Stress Model) turbulence model are run in CFX. The use of the BSLRSM is justified in order to assess the influence of the secondary motions when compared with the results obtained by the SST model.

Regarding the near wall modelling: for all meshes the boundary layer profiles are successfully solved (no use of wall functions), i.e., all meshes have a dimensionless wall distance y^+ under 3 for the SST model, and under 1 for the BSLRSM. Furthermore, at least 20 cells are within the boundary layer, having an expansion ratio of less than 1.2. The mesh for the simulations with the hole plate contains 17 million cells for the whole flow conditioning region. The number of cells for the simulations without the hole plate is 2.5 million cells for the hole flow conditioning region. This huge difference can be understood when considering that 215 holes with a diameter of 1.6 mm are in the hole plate. Furthermore, the whole simulated flow conditioning section is 3.6 m long. The hole plate optimization is performed with the SST model, because neither qualitative nor quantitative differences are present for between the SST model and the BSL-RSM model for the hole-plate region.

The residuals convergence criteria are set to 10^{-9}. Nevertheless, the fact that convergence of numerical residuals cannot be taken as a criterion for steady state cases is self-evident and well known. Hence, the main convergence criteria for all simulations are random located points at the domain´s outlet for all three velocity components and the averaged pressure at the domain´s inlet. Once all these variables are stable, the simulation is stopped. At least second order schemes are used for every variable and every calculation. No convergence problems are observed in the simulations. For every single used mesh, mesh independency is achieved. All typical mesh-quality indicators found in the literature (orthogonal quality, skewness, aspect ratio etc.) are satisfied.

The properties for sodium are taken at 150 °C, based on the recommendations of Sobolev [13]. The volume flow rate is 3 m³/h (KASOLA has a maximum flow rate of 150 m³/h). A fully developed turbulent velocity profile is taken as an inlet velocity condition. Also, fully developed turbulent kinetic energy and turbulent dissipation rate profiles are taken as inlet boundary conditions for the SST model. For the BSL RSM model, the Reynolds stresses are given as an input at the inlet. These profiles are taken from previous simulations at Re = 23000, taking the laminar equivalent hydraulic diameter [11] as the characteristic length.

In Table 1, the validation efforts are presented. Very similar values can be seen for the predicted pressure drop and maximum velocity in the turbulent boundary layer profile compared with the simulation. From Table 1 it can also be seen, that – contrary to what would be expected – the pressure drop along the rounded corner duct is higher than for the sharp corner case. This is due to the cross-section area reduction when taking the rounded corners. Having a constant volume flow rate, has the consequence of a higher bulk velocity, which slightly increases the pressure drop. It is interesting to note that the SST model gives a lower pressure drop than the BSLRSM model, which is expected due to the secondary motions not considered in the SST model

The results for the simulation with the BSLRSM model comparing the 90° sharp corner rectangular duct with the rectangular profile duct with rounded corners are shown in Figure 2. No major qualitative differences between both cases are found. Also, the quantitative values agree over all. It must be recalled, that these simulations are done with a corner radius of 10 mm for the rectangular duct with rounded corners, in order to accentuate the behaviour of the rounded corners. The original geometry has an inner corner radius of 5 mm, so that the effect of the rounded corners in the experiment will be even smaller.

Table 1 Values for pressure drop across a duct of 3600 mm length and maximal velocities in a turbulent boundary layer using empirical correlations and RANS CFD models

	Empirical correlations		Sharp 90° corners		Rounded corners	
	Techo	Colebrook	SST	BSLRSM	SST	BSLRSM
Δp [Pa]	40.9	41.8	39.7	41.7	40.8	43.1
U [m/s]	-	0.286	0.290	0.280	0.294	0.284

In the following, the results regarding the implementation of hole plates are discussed. The hole plate is placed at the end of the round-to-rectangular adapter, i.e., at the inlet of the rectangular duct. For every studied case, i.e. with and without hole plate, three inlet velocity boundary layer

profiles are implemented: fully developed, linear and swirl. This is done to study the real impact of the hole plate for "erasing" velocity boundary layer profile distortions from upstream components. All simulations are performed with both SST and BSLRSM turbulence models.

The results regarding the inlet boundary conditions can be seen in Figure 3. No matter what inlet boundary condition is implemented, the hole plate erases the velocity boundary layer distortion immediately after the adapter, in contrast to the case without a hole plate. Nevertheless, the flow conditioning section is long enough to diminish these upstream generated distortions, independently of the presence of the hole plate.
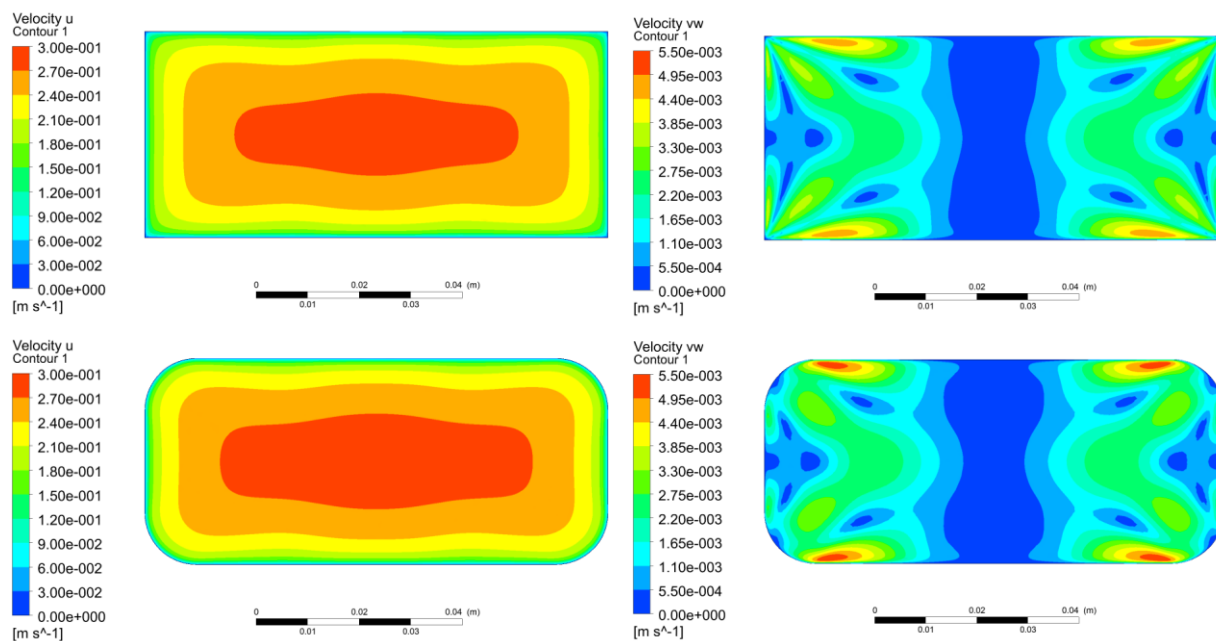
Figure 2: Velocity contours for the U-component (left side) and the vector sum of the V and the W components (secondary motions).

Contrary, when taking the SST model, i.e., without considering secondary motions, it cannot be stated that this will be valid for the case without a hole plate, because, when taking two samples of the velocity boundary layer very close to the outlet of the computational domain, one can see that the boundary layer is still varying (these results are not shown due to a of space limitation). When watching this behavior, it is plausible to think that the secondary motions, due to their momentum distribution effect [14], could be a flow conditioner by themselves. It is also very interesting to mention, that one has to be careful with the concept of "entry length". According to Kakac [11], the entry length is defined as the point where both boundary layers of a Poiseuille-flow meet at the center line of a duct. This does not mean, that the velocity profile is fully developed, though; at least in a rectangular duct, where the secondary motions will still act as momentum distributors for quite a few hydraulic diameters [14].
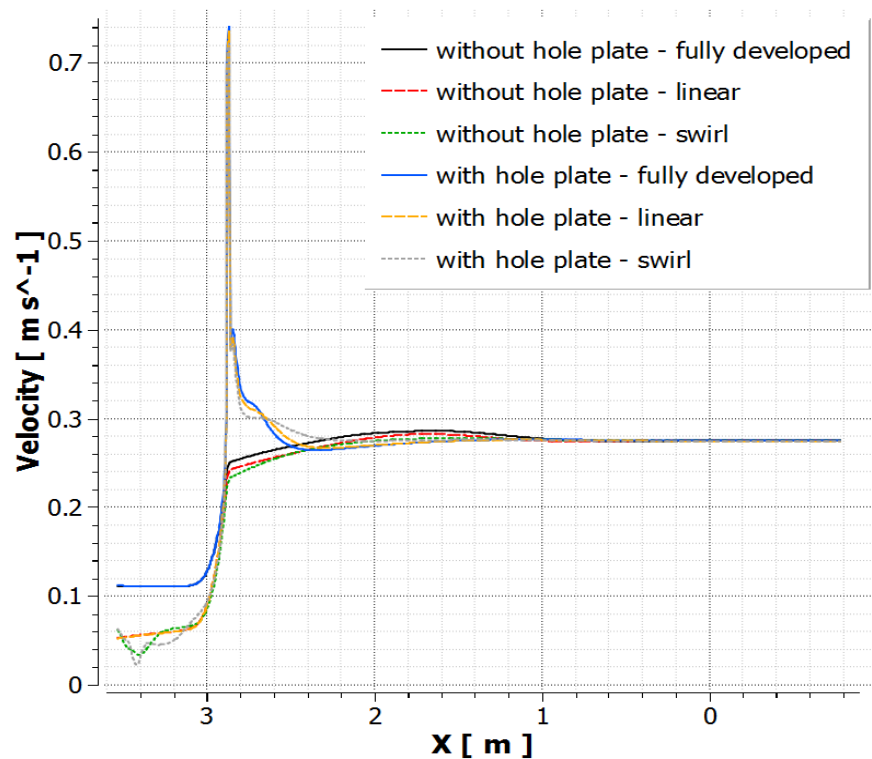
Figure 3: Velocity development along the X-axis of the flow conditioning section for different inlet velocity boundary layer profiles and for both studied flow conditioning setup cases: with and without hole plate.

This is the reason why the typical rule-of-thumb of 20-25 hydraulic diameters predictions for entrance length for turbulent flows do not apply for our case, considering that we want to have a fully developed turbulent boundary layer profile at the backward facing step. Melling and Whitelaw [14] show that in their experiment, a constant centerline axial velocity in a rectangular duct is not achieved within 35 hydraulic diameters. Those values agree with the shown CFD results (Figure 3). This means that implementing flow conditioning hardware, in spite of having a 63 hydraulic diameter long flow conditioning section is not an overkill. This is also supported by past experiences in liquid metal experimental facilities at KIT.

4.   Complimentary direct numerical simulations

The direct numerical simulations (DNS) of the backward facing step within the SESAME project are performed by the Jožef Stefan Institute. The BFS geometry is simulated in three dimensions without the rounded corners. For the time being, only fluid flow features are investigated, without the thermal properties. The thermal properties, together with solid walls will be added in the near future.

The DNS is performed with the open source code NEK5000 [15]. This code is developed by one of the partners in the SESAME project, Argonne National Laboratory. NEK5000 is an implementation of the spectral element method, which is a hybrid method between finite element method and a spectral method. On the one hand, similar to the finite element method, the domain

is divided into finite elements. On the other hand, similar to the spectral method, the solution within each element is obtained with a spectral method. Patera introduced the spectral element method in the year 1984 [16].

The spectral element method retains the quick convergence rate of the spectral method, but also inherits the ability to simulate irregularly shaped geometries from FEM. The elements also become the unit, by which we can compute in parallel.

The BFS geometry differs a little from the geometry of the experiment. It does not contain the rounded edges that will be present in the experiment. Additionally, the expansion ratio of the step, which is the ratio of the area of the outflow and the area of the inflow, is a bit lower than in the experiment. The DNS are performed with the expansion ratio of 2. In the dimensionless units, the simulated BFS geometry had $12 \times 2 \times 4$ units before the step and $22 \times 4 \times 4$ afterwards. The Courant number was kept below 0.3 during the simulation.

The BFS domain is divided into four regions with around 60,000 elements. Within each element, 7 collocation points are used in each direction. The whole domain has around 13 million unique points, in which equations are solved. Equations that are solved are the dimensionless Navier-Stokes equations for incompressible fluid. The fluid properties are considered constant. A more detailed description of the method, the equations, the geometry and results is provided in a separate paper on DNS of BFS geometry at the NURETH 17 conference [17].

The BFS geometry, that is simulated, has walls at all sides of the domain, except for the inflow and outflow. No-slip boundary condition is applied at the walls. At the outflow zero pressure is applied. Small corrections are added to disallow for any back flow into the computational domain that might occur. These corrections make the fields in at least 4 dimensionless units to the outlet slightly non-physical. At the inflow, a more complicated boundary condition is imposed. First, the values of the velocity from a parallel plane and 6 dimensionless units downstream to the inflow are taken. Then, the stream-wise velocity component is normalized, so that its average throughout the plane is equal to one. This planar velocity field is then imposed as the inflow boundary condition.

The simulations are performed with a Reynolds number of 15040, based on bulk velocity and hydraulic diameter concept. The calculated friction Reynolds number Re_τ of the simulation before the step is equal to about 330. The particular results shown here are calculated for approximately four days on a machine with 360 CPU cores. The whole simulation made 500 thousand time steps and around 550 dimensionless time units.

In Figure 4 the averaged stream-wise velocity component is shown in comparison to experimental data. These results are averaged for about 360 dimensionless time units or about 320 thousand time steps. The maximum average velocity in the stream-wise direction is achieved in the channel before the step and is equal to about 1.23 dimensionless velocity units. After the step, the maximum velocity in the stream-wise direction decreases (note that in Figure 4 the distances between profile lines before the step and after the step are not the same). Due to the fluid being incompressible and the expansion ratio of the BFS geometry equal to 2, the average velocity through the cross-section drops to 0.5.
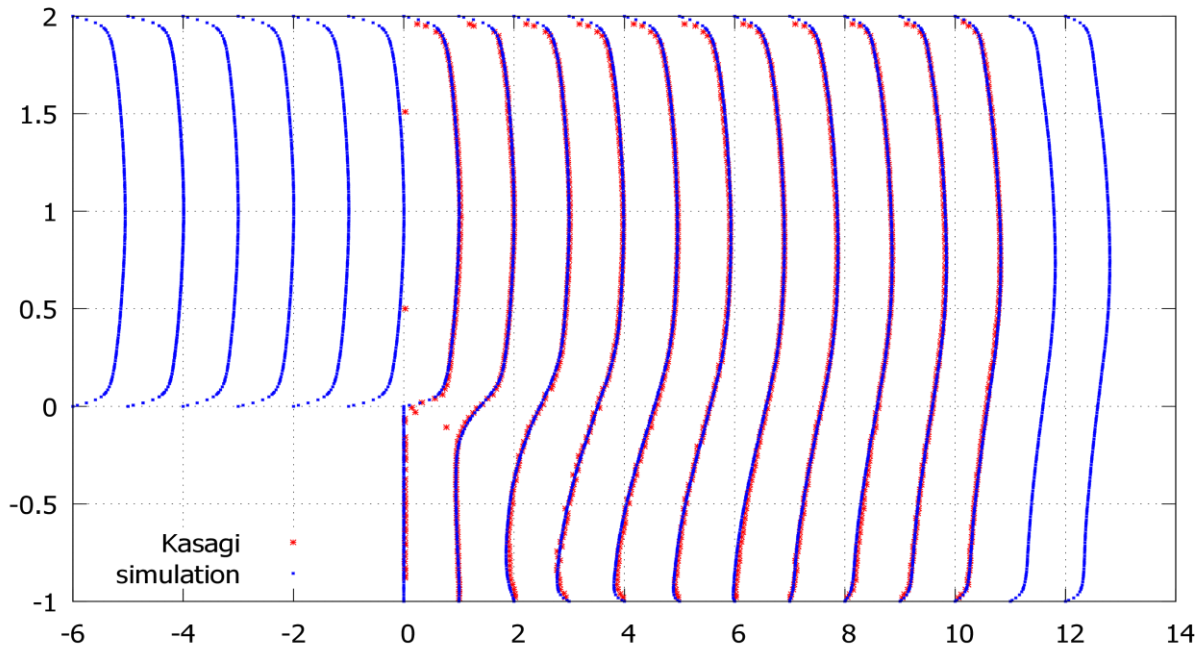
Figure 4: The averaged stream-wise velocity component throughout the middle plain of the domain is shown

In Figure 5 the three dimensional shape of the path-lines behind the step are shown. The path-lines from the middle and upper parts at the inflow are almost straight to the outflow (these are not shown in the figure). However, they do not fill the whole outflow region, but just about 3/4 of the outflow height. The remaining quarter of the outflow is filled with path-lines from the bottom corners of the inflow. These can have multiple loops. Here, only selected path-lines that are not too complex are shown to sketch the flow pattern after the step. Behind the step, it is visible that a vortex is formed and in the lower part of the domain, the fluid is flowing in the opposite direction to the main stream. In fact, there is also a second vortex in the lower corner of the step. This can be observed in Figure 6. This figure shows the average stream-wise velocity field at the bottom wall after the step.

The contour marks where the stream-wise velocity changes the direction. At the left side of Figure 6 is the backward facing step and at the right side is the outflow. Following from right to left, the stream-wise velocity at the outflow is in the direction of the outflow. Then it changes direction and the stream-wise component points in the opposite direction of the general flow. Near the step wall, it changes the direction again. The magenta line in Figure 6 (at x ~ 15) marks the calculated position of the average reattachment zone. This distance is equal to 15.3 dimensionless units behind the step. It was calculated from the time-averaged velocity that was averaged in the z-direction at the bottom of the domain behind the wall between the dotted lines. The details of this calculation are also given in a separate paper [17].
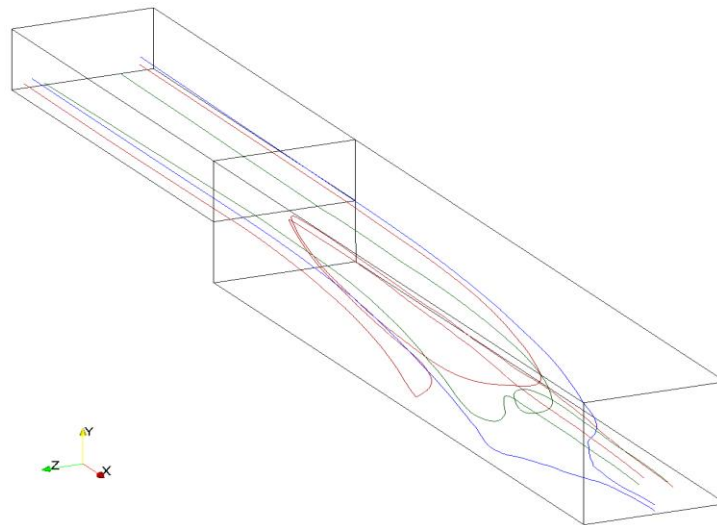
Figure 5: Selected path-lines of the average flow
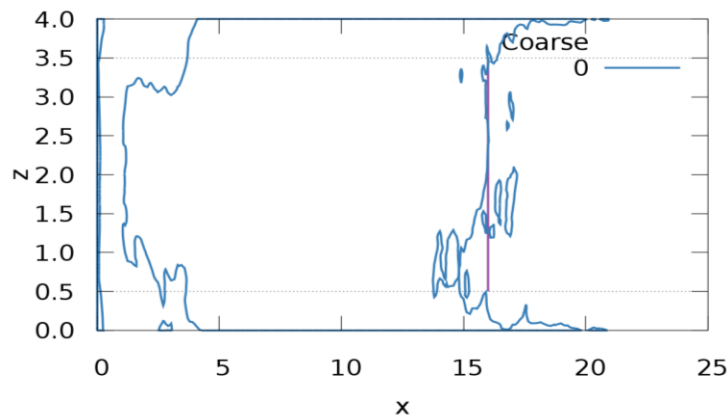
Figure 6: Flow reattachment zone at the bottom of the channel behind the step. The magenta colored line shows the approximate location of the reattachment zone.

5.   Complimentary large eddy simulations

Within the SESAME project, Large Eddy Simulations (LES) of turbulent flow over a BFS are ongoing at KIT. In this section a report is given on first LES calculations performed for incompressible, isothermal flow over a BFS. Because the experimental activities at KIT and the DNS calculations at JSI are ongoing, the first LES simulations are tested against the results from the literature. Data by Kasagi and Matsunaga [18] for steady-state isothermal turbulent flow over the BFS with water as fluid are chosen for comparisons with LES results. The Reynolds number, based on the centerline velocity U_c and step height H is 5540 at the Kasagi and Matsunaga experiment and corresponds to the Reynolds number chosen at the KASOLA experiment. LES is performed using the open source CFD toolbox OpenFOAM.

The standard dynamic one-equation turbulent subgrid scale (SGS) model is applied (see e.g. Ghosal, Lund, Moin and Akselvoll [19]). The calculated BFS geometry is given in the following. The inlet cross section height is 81 mm and the step height H is 41 mm. The channel width is 122 mm and the length downstream of the step is 800 mm. Apart of the streamwise length, the computational domain corresponds to the experiment by Kasagi and Matsunaga and further details on the experimental setup can be found in [18].

The computational grid consists of about three million hexahedral elements. No-slip boundary conditions are applied for all walls. Walls are resolved and the overall maximum y^+ is less than one. The outlet boundary condition (BC) is inlet-outlet boundary which is defined as a switch between the Dirichlet and Neumann BC depending on the velocity vector orientation at the outlet patch. The advective BC is tested at the outlet. If a good choice of constant advective velocity is provided, being the main disadvantage of advective BC, no difference in the results are observable. The inlet section of the computational domain is chosen as 3.5 times H long in the streamwise direction. An inlet box of 2.5 times H length in the streamwise direction with periodic boundary conditions is introduced into the inlet section to provide fully developed inlet boundary conditions. Figure 7 shows the comparison between the experimental results [18] for the mean streawise velocity at the step and the LES results. The LES results are evaluated at the step, at the end of the cyclic box (position at 2.5 times H stream wise from the inlet patch), and at the position 2 times H (within the periodic box). All simulation results are completely collapsing and in very good agreement with the experiment. However, there is a small discrepancy between the experimental and numerical results at the edge of the upper boundary layer which is probably due to the near wall resolution of the upper wall.

Figure 8 shows the comparison between the experimental and numerical results for the mean streamwise velocity profiles after the step. Small discrepancy within the recirculation zone can be observed. It can be expected that this discrepancy will be resolved by further numerical integration in time and longer averaging period. At the position 10 x/H a small discrepancy over the entire channel between the experimental and numerical results can be observed. This is not only due to the integration time but also to the short calculation domain as compared to the streamwise length of the experiment (1.7 m). However, the first calculations presented here are intentionally chosen for the short domain in order to minimize the number of cells.

Because the LES is isothermal, i.e. no heat flux turbulence model and therefore no Pr effects on simulation results exist. The aim of the LES study is to prove the capability of the dynamic eddy viscosity model for simulations of hydraulic fields at similar Reynolds numbers as in the KASOLA liquid sodium experiment. Furthermore, the results are compared with independent experimental results from literature. The geometry of the Kasagi et al. experiment, which is used for LES comparisons, is slightly different as the KASOLA experimental set-up. Hence, direct comparisons will not provide additional clarity for the moment
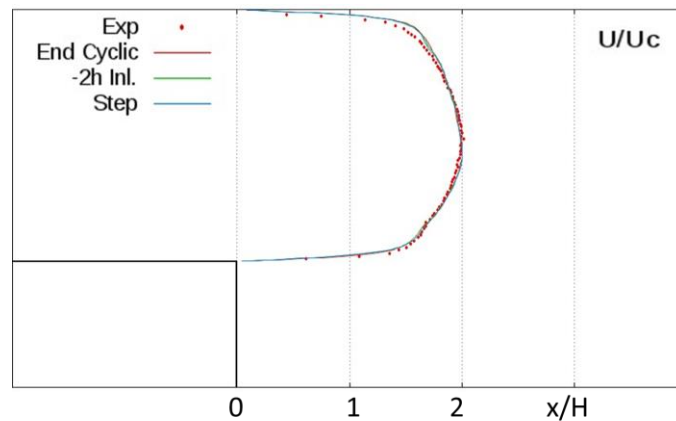
Figure 7: Streamwise mean velocity distribution: symbols, experimental results at the step [18];
lines are simulation results
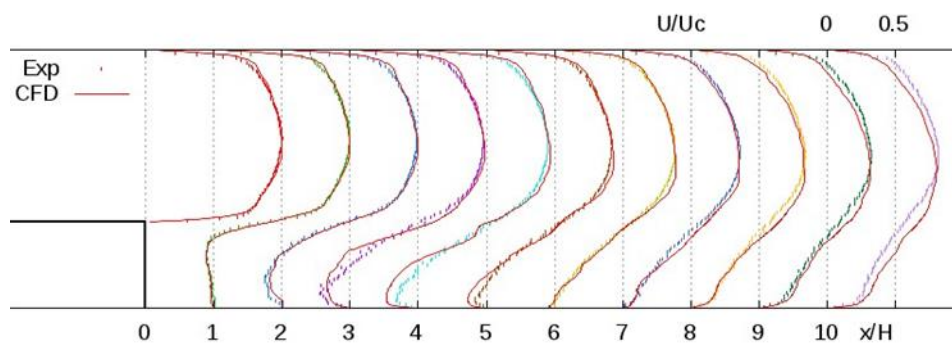
Figure 8: Streamwise mean velocity distribution: symbols, experimental results [18]; lines are
simulation results

6.   Summary

In this paper a qualitative evaluation of a BFS experiment is presented. This BFS is made of two stainless steel sections, a rectangular section with the external dimension of 100 x 50 mm before the BFS and a quadratic section with the external dimensions of 100 x 100 mm. For both sections the wall thickness is 5 mm. The first section has a length of 3600 mm, while the second section is 2000 mm long. Due to practical reasons, the sections are made with rounded corners.

Isothermal CFD investigations are conducted to evaluate the influence of rounded corners, as compared to straight 90°, on the flow in general and the secondary motions in particular. The investigation show that no qualitative differences exist between straight 90° corners and rounded corners. In a further step, the entrance length is evaluated. In the present configuration, a flow rectifier is installed by means of a hole plate. This hole plate is 3600 mm upstream of the BFS, which is equivalent to roughly 63 hydraulic diameters. The performed investigation considers different inlet velocity profiles, like linear, swirl or flat profiles. In all cases 3600 mm are enough

to establish developed flow conditions. As a supporting measure, DNS investigations are performed. With this investigation, the flow after the step is evaluated. Representative flow paths are shown, visualizing the recirculation zone and the reattachment points of the flow. This information is helpful for, among others, the positioning of the measurement devices. Complementary isothermal large eddy simulations are performed. LES requirements on fully developed inflow conditions are evaluated. Results show very good performance of the homogeneous dynamic one equation SGS model.

7.   Acknowledgement

8.   Nomenclature

c_p	Specific heat capacity
h	Heat transfer coefficient
k	Thermal conductivity
δ	Film thickness
Γ	Film flow rate
η	Dynamic viscosity
Nu	Nusselt number
Pr	Prandtl number
Re	Reynolds number

9.   References

[1]   W. Oberkampf, "Verification and Validation in Computational Fluid Dynamics", SANDIA Report eSAND2007-0853, February 2007.

[2]   F. Roelofs, A. Shams, A. Batta, V. Moreau, I. Di Piazza, A. Gerschenfeld, P. Planquart and M. Tarantino, "Liquid Metal Thermal Hydraulics, State of the Art and Beyond: The SESAME Project", Proceedings of the European Nuclear Conference, Warsaw, Poland, 2016 October, 9-13.

[3]   F. Roelofs, A. Shams, I. Otic, M. Boettcher, M. Duponcheel, Y. Bartosiewicz, D. Lakehal, E. Baglietto, S. Lardeau and X. Cheng, 2015a. "Status and perspective of turbulence heat transfer modelling for the industrial application of liquid metal flows", Nuclear Engineering & Design, Vol. 290, 2015, pp. 99-106.

[4]   F. Roelofs, A. Shams, J. Pacio, V. Moreau, P. Planquart, K. van Tichelen, I. Di Piazza and M. Tarantino, "European Outlook for LMBR thermal hydraulics", Proceedings of the 16th International Topical Meeting on Nuclear Reactor Thermal Hydraulics, Chicago, IL, USA, 2015 August 30 – September 4.

[5]   A. Shams, F. Roelofs, E. Baglietto, S. Lardeau and S. Kenjeres, "Assessment and calibration of an algebraic heat flux model for low-Prandtl fluids", International Journal of Heat and Mass Transfer, Vol. 79, 2014, pp. 589–601.

[6]   L. Carteciano and G Groetzbach, "Validation of turbulence models for a free hot sodium jet with different buoyancy flow regimes using the computer code FLUTAN", FZKA Report 6600, Research Center Karlsruhe, 2003.

[7]   W. Hering, R. Stieglitz, A. Jianu, M. Lux, A. Onea, S. Scherrer and C. Homann, "Scientific program of the Karlsruhe Sodium Laboratory (KASOLA)", Proceedings of the International Conference on Fast Reactors and Related Fuel Cycles, Paris, France, 2013, March 4–7.

[8]   R.I. Loehrke and H.M. Nagib, "Experiments on management of free-stream turbulence", AGARD Report 598, 1972.

[9]   E.M. Laws and J.L. Livesey, "Flow through screens", Annual Review of Fluid Mechanics, Vol. 10, 1978, pp.247-266.

[10]   P.E. Roach, "The generation of nearly isotropic turbulence by means of grids. International Journal of Heat and Fluid Flow, Vol. 8, No. 2, 1987, pp 82-92.

[11]   S. Kakac, R.K. Shah and W. Aung, "Handbook of Single-Phase Convective Heat Transfer", John Wiley and Sons Inc, 1986.

[12]   F. White, "Fluid Mechanics", 8th edition, Mc Graw Hill Education, 2015.

[13]   V. Sobolev, "Database of thermophysical properties of liquid metal coolants for GEN-IV", Scientific Report SCK-CEN-BLG-1069, 2010.

[14]   A. Melling and J.H. Whitelaw, "Turbulent flow in a rectangular duct", Journal of Fluid Mechanics, Vol. 78, part 2, 1976, pp. 289-315.

[15]   P.F. Fischer, J.W. Lottes and S.G. Kerkemeier, "nek5000 Web Page", 2008.

[16]   A.T. Patera, "A Spectral Element Method for Fluid Dynamics: Laminar Flow in a Channel Expansion", Journal of Computational Physics, No. 54, 1984, pp. 468–88.

[17]   J. Oder and I. Tiselj, 2017. "Direct Numerical Simulations of Sodium Flow over a Backward Facing Step." Proceedings of the 17th International Topical Meeting on Nuclear reactor Thermal Hydraulics, Xi'an, China, 2017 September 3-8.

[18]   N. Kasagi and A. Matsunaga, "Three-dimensional particle-tracking velocimetry measurement of turbulence statistics and energy budget in a backward facing step flow", International Journal of Heat and Fluid Flow, Vol. 16, 1995, pp. 477-485.

[19]   S. Ghosal, T.S. Lund, P. Moin, and K. Akselvoll, "A dynamic localization model for large-eddy simulation of turbulent flows", Journal of Fluid Mechanics, Vol. 286, 1995, pp. 229-255.